Determination of Ag domain populations on Cu(111) using directional Auger and directional elastic peak electron spectroscopies

Marek Nowicki*
Institute of Experimental Physics, University of Wrocław, Pl. Maxa Borna 9, 50-204 Wrocław, Poland
(Received 2 February 2004; revised manuscript received 31 March 2004; published 30 June 2004)

The Auger signal and the intensity of elastically backscattered electrons were measured as a function of the incidence angle of the primary electron beam to find the crystalline structure of ultrathin Ag layers on the Cu(111) surface. Experimental profiles were compared with theoretical data obtained with the use of single scattering cluster (SSC) calculations for clean and covered Cu(111). Auger scans for Ag MNN transition and elastic peak profiles exhibit intensity maxima corresponding to two mutually rotated Ag(111) domains. Different domain populations were found by an R-factor analysis, which can be rationalized by the miscut of the Cu(111) sample and the resulting step orientation.

DOI: 10.1103/PhysRevB.69.245421 PACS number(s): 68.55.−a, 61.18.−j, 61.14.−x

I. INTRODUCTION

Information about the morphology and atomic structure of adlayers on substrates is useful in the investigation of a crystal growth. The sites occupied by adatoms play a crucial role in governing the atomic structure of adlayers. For the first monolayer one can consider three structures: pseudoepitaxy, pseudomorphy, and reconstruction.[1,2] The growth on the first layer leads to the formation of a film. Its crystalline structure and orientation with respect to the substrate depend on the stacking sequence at the interface. Different stacking sequences cause the nucleation of rotated and unrotated domains.

The investigation of the atomic structure of adsorbed layers requires structurally and chemically sensitive experimental techniques. In x-ray photoelectron diffraction (XPD) and Auger electron diffraction[3–7] an anisotropic emission from crystalline samples is observed. Due to the forward scattering[8] the straightforward identification of the crystalline order of the first atomic layers is possible.

Forward scattering takes place not only for electrons emitted from the crystalline sample but also for the primary electrons striking the sample. Examples of incident beam experiments can be found in a number of papers.[9–18] The so-called directional Auger and directional elastic peak electron spectroscopies (DAES and DEPES, respectively) were proposed,[14] where the dependence of the angle-integrated electron emission on the primary electron beam direction was used. In these experimental techniques the Auger signal and the intensity of elastically backscattered electrons are measured, with the use of a retarding field analyzer (RFA), as a function of the incidence angle of the primaries. Due to the large acceptance angle of the analyzer (104°), about 40% of all emitted electrons at a given energy were detected. The integration of the signal over the large acceptance angle of the collector ensures that the influence of the angular distribution of electron emission on the measured profiles is negligible in comparison with the diffraction effects of the primary beam. The intensity maxima observed experimentally reflect the crystalline structure of samples.[14,16,19–23] In the light of this fact DAES and DEPES are closely related to XPD.[24] DAES and DEPES extend the experimental utility of an RFA analyzer, which is commonly used for low energy electron diffraction (LEED) pattern observations and Auger electron spectroscopy (AES).

In this paper, DAES and DEPES were used to recognize Ag domains with different orientations with respect to the Cu(111) substrate. Single scattering cluster (SSC) approximation was used to calculate theoretical polar scans. To obtain quantitative information concerning the domain populations, reliability factors (R-factors) were calculated for the comparison of theoretical and experimental profiles.

II. EXPERIMENT

All measurements were performed in an UHV system equipped with a RFA analyzer with a working pressure of typically 10^{-10} mbar. In DAES and DEPES the primary electron beam was directed onto the crystalline sample.[14] By modulating the voltage of the grids it was possible to measure an Auger signal in the $dN(E)/dE$ mode and the peak height of elastically scattered electrons in the $N(E)$ mode.

The Cu(111) sample was mounted on a standard manipulator enabling independent rotation around two axes, one lying in the sample surface and the other perpendicular to this surface. The required azimuth of the sample surface was chosen by rotating the sample around the axis perpendicular to the Cu(111) plane. The incidence angle of the primary electron beam was changed by rotation around the axis parallel to the sample surface. DAES and DEPES profiles were recorded for different primary beam electron energies E_P.

The Cu(111) crystal was cleaned by annealing at 900 K and by simultaneous potassium ion bombardment from a zeolite source.[25] After cleaning, which was repeated when necessary during measurements, no evidence of sulphur, carbon, and potassium was detected by AES. Silver was evaporated from a quartz cup surrounded by a tungsten resistive heater. During the silver evaporation, the silver flux was perpendicular to the Cu(111) surface and the incidence angle of the primary electron beam was equal to 60°. In this system the silver deposition and the simultaneous recording of the Auger peak heights were possible. Kinetics of h_{Cu} (62 eV) and h_{Ag} (360 eV), where the h_{Cu} and the h_{Ag} are Auger peak

heights for Cu and Ag, respectively, were recorded by a computer during the continuous silver deposition.[26] The coverage of silver was estimated independently from the kinetics and with the use of a quartz oscillator placed close to the sample.

III. SSC THEORY

To describe the primary beam diffraction effects the single scattering cluster approximation was used. I take into account that the incident electrons undergo the same elastic scattering as the emitted photoelectrons in XPD. Therefore, DAES and DEPES can be considered as time reversals of XPD,[24] although no photons are associated with emitted electrons.

The electron wave field emanating in a solid is strongly scattered by atoms, which results in a coherent interference of scattered components. The interference depends strongly on the scattering angle and wavelength, which affect phase shifts among direct and scattered waves, as well as on the distance between atoms and on the atomic number Z. As a result of the above interference the maximum of the scattering amplitude is observed along the forward direction.[8] Thus, forward focusing of electrons occurs at kinetic energies of about a few hundred electronvolts.

Taking into account the above considerations electrons striking the sample are channelled into cones of several degrees in width along the incidence direction. The tips of the cones are located on atoms or between them, depending on the incidence angle. Thus, the illumination of a given atom depends on the primary beam direction. As a result, the probability of electron-hole creation, which results in the Auger electron emission, and of elastic scattering events depends strongly on the incidence angle. In view of this fact an increase of both the Auger signal and the elastic peak height is expected when the collimated beam passes through the close packed rows of atoms.

In SSC calculations the incident wave is considered to be a plane wave with the propagation vector $\boldsymbol{k}$ and only single scattering of the primary electrons is taken into account. Under these assumptions the wave function of the elastically scattered electrons at any site $\boldsymbol{r}$ in the crystal can be written as[24,27]

$$\Psi(\boldsymbol{k},\boldsymbol{r}) = e^{i\boldsymbol{k}\boldsymbol{r}}\left[e^{-r_z/\Lambda\ \cos\ \Theta} + \sum_j e^{-i\boldsymbol{k}\boldsymbol{d}_j} e^{-r_{zj}/\Lambda\ \cos\ \Theta} e^{-d_j/\Lambda} f_j(\boldsymbol{k},\boldsymbol{d}_j,T)\frac{e^{i\boldsymbol{k}\boldsymbol{d}_j}}{kd_j}\right]. \tag{1}$$

The sum extends over all scattering atoms j in the crystalline sample.

In Eq. (1) the phase changes associated with pathlength differences and scattering are considered. Λ is the inelastic mean free path of primary electrons, $r_z/\cos\Theta$ and $r_{zj}/\cos\Theta$ are paths inside the solid of unscattered but attenuated waves at sites $\boldsymbol{r}$ and $\boldsymbol{r_j}$, respectively, Θ is the incidence angle, $\boldsymbol{d_j} = \boldsymbol{r} - \boldsymbol{r_j}$, T is the absolute temperature, and $f_j(\boldsymbol{k},\boldsymbol{d_j},T)$ is the scattering factor of electrons scattered by atom j. The latter factor involves the scattering amplitude, the temperature dependent phase shifts calculated in a muffin-tin approximation with the use of the Pendry mufpot-program,[28] and the curved wave fronts at site r.[29] The complex factor f_j can be expressed as[30]

$$f_j(\boldsymbol{k},\boldsymbol{d_j},T) = \sum_{l=0}^{\infty} t_l^j(T) c_l(kd_j)(2l+1)P_l(\cos\ \theta_{kd_j}). \tag{2}$$

where t_l^j is the temperature dependent scattering t-matrix, which describes the scattering amplitude and the vibrational properties of the atom j,[28] c_l is the polynomial factor that multiplies the asymptotic form of the spherical Henkel functions, P_l is the lth Legendre polynomial, and Θ_{kd_j} is the scattering angle between vectors $\boldsymbol{k}$ and $\boldsymbol{d_j}$.

The Auger signal and intensity of elastically backscattered electrons integrated over the large acceptance angle of the analyzer are proportional to the sum of the primary beam intensities over all atomic sites S in the crystal weighted with the escape probability of the outcoming electrons A[24,27]

$$I(k) = \sum_S |\Psi(\boldsymbol{k},\boldsymbol{r_s})|^2 A\left(\frac{r_z}{\Lambda_{\text{out}}}\right). \tag{3}$$

The value of A, which takes into account the damping of emitted electrons along their way toward the surface, is governed by the distance of an emitter from surface r_z and the inelastic mean free path of outcoming electrons Λ_{out}. The integration of the inelastic damping $e^{-r_z/\Lambda_{\text{out}}\ \cos\ \phi}$ over all possible emission angles ϕ leads to the formula

$$A\left(\frac{r_z}{\Lambda_{\text{out}}}\right) = \int_1^{\infty} \frac{e^{-r_z\cdot t/\Lambda_{\text{out}}}}{t^2} dt, \tag{4}$$

where t is equal to $1/\cos\phi$.

Based on Eqs. (1)–(4) DAES and DEPES profiles can be calculated taking appropriate energies of primary and emitted electrons, and associated with their values inelastic mean free paths, and weights of "emitters." In DAES and DEPES the information depth about the atomic order depends on the primary beam energy E_P and r_z/Λ_{out} ratio. For example Λ for primary electrons at $E_P = 1.0$ keV was chosen to be 14.9 Å. For emitted electrons and Ag MNN transition at $E_P = 360$ eV Λ_{out} was 8.9 Å. Both methods are surface sensitive and DAES contains additionally chemical information.

IV. RESULTS AND DISCUSSION

In a RFA analyzer the primary energy E_P ranges from several electron volts in the LEED mode to 3 keV in the AES regime. Forward focusing of electrons takes place for $E_P \geqslant 500$ eV, therefore the influence of diffraction effects of primaries in a solid on the recorded signal in DAES and DEPES can be investigated. In Fig. 1 the experimental and theoretical DEPES and DAES profiles from Cu(111) for $E_P = 1.2$ keV are presented. Well-distinguished intensity maxima are observed for incident angles corresponding to the [001], [112], and [110] close packed atomic directions in the Cu(111) sample, which gives straightforward identification of the crystalline structure. Nearly the same signal de-

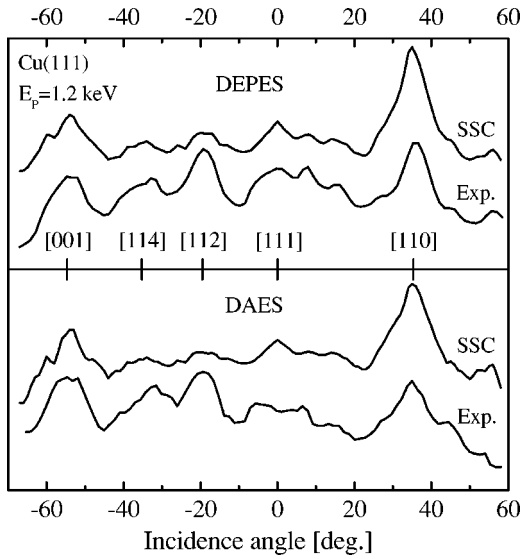

FIG. 1. Experimental and theoretical DEPES and DAES ($M_{2,3}VV$) profiles from Cu(111) in the $[11\bar{2}]$ azimuth for E_P =1.2 keV.

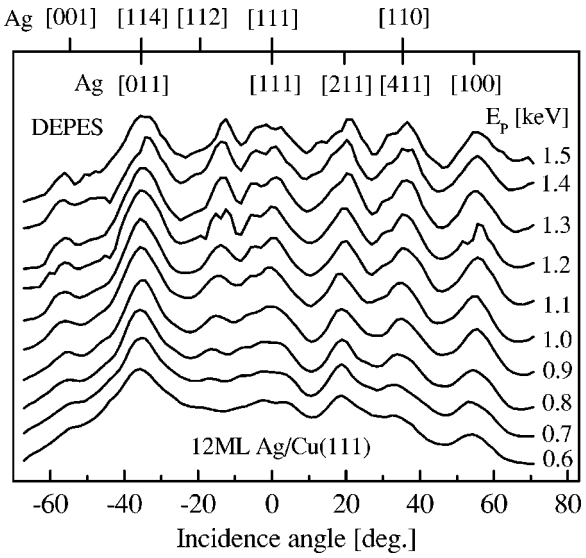

FIG. 2. Experimental DEPES profiles for 12 ML of Ag on Cu(111) in the $[11\bar{2}]$ azimuth of Cu for different primary beam energies E_P.

pendence on the incident angle is observed for both experimental scans, which is expected for DAES and DEPES profiles recorded at the same primary beam energy. Intensity maxima are well reproduced by SSC theory, as it was found in Refs. 21, 22, and 24, including signal fluctuations observed between the [111] and [110] directions. The overall agreement of the SSC data with the experimental results is of similar quality to that found in XPD.[24] For Ag/Cu(111) a pseudoepitaxial, corrugated $p(10\times10)$ structure of the Ag monolayer was theoretically predicted.[2] Scanning tunnel microscope images show two-dimensional close packed Ag islands, with slightly deformed structure.[31] AES kinetics[32–36] recorded during continuous silver deposition show that the Ag growth on Cu(111) is not of the pure Frank-van der Merwe type.[26]

Experimental DEPES profiles for 12 ML of Ag on Cu(111) in the $[11\bar{2}]$ azimuth of Cu and different E_P values are presented in Fig. 2. The diffraction conditions of the primary electrons depend on the electron beam energy. Therefore, changes of the measured signal are expected when the E_P value is altered. Forward focusing of primaries takes place along the close packed rows of atoms. Thus, well-distinguished intensity maxima at −35°, 19.5°, and 55° correspond to [011], [211], and [100] directions of the Ag(111) crystal, respectively. For other directions, e.g., [111], the changes of the measured signal with energy are noted. The maxima at −55° and −19.5° corresponding to the [001] and [112] directions of the Cu substrate (Fig. 1) are not present in the adsorbate profiles. The above results demonstrate that the Ag layer is rotated by 180° with respect to the Cu(111) substrate. This rotation can be rationalized by the ABCBAC stacking sequence at the Cu-Ag interface.

In view of the fact that a qualitative correspondence between experimental and theoretical data was found, a R-factor analysis[37] can be used to obtain quantitative information concerning the populations of rotated and unrotated domains in the Ag adsorbate. The experimental polar profiles were compared with a linear combination of the results obtained from SSC calculations for two possible domains mutually rotated by 180°

$$I_{Th} = \sum_{i=1}^{2} n_i I_{\mathrm{Th},i}, \tag{5}$$

where $I_{\mathrm{Th},i}$ is the intensity calculated for domain i weighted by its population n_i. Each n_i value was varied with 1% steps while fulfilling the $\Sigma_{i=1}^{2} n_i = 1$ condition.

In order to eliminate the intensities and take into account relative positions of peaks the logarithmic derivative $L = I'/I$ was calculated, where I and I' are intensity and its

TABLE I. Populations of two Ag(111) domains on Cu(111) obtained from DAES and DEPES for different primary beam energies E_P. The mean values of populations are $\overline{n_1}$=71±3% and $\overline{n_2}$ =29±3%.

	DAES		DEPES	
E_P [keV]	n_1 [%]	n_2 [%]	n_1 [%]	n_2 [%]
0.6	69	31	69	31
0.7	73	27	78	22
0.8	77	23	75	25
0.9	78	22	70	30
1.0	69	31	67	33
1.1	69	31	68	32
1.2	75	25	69	31
1.3	71	29	70	30
1.4	70	30	68	32
1.5	73	27	72	28
2.0	69	31		

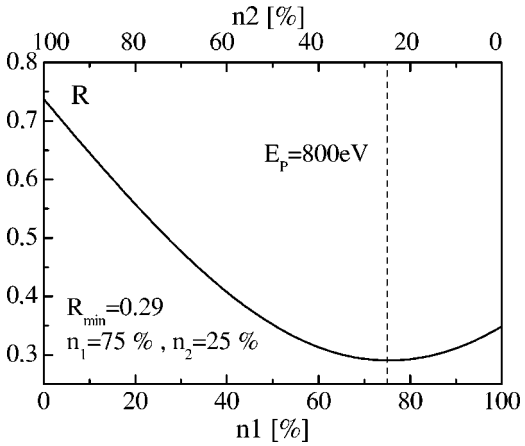

FIG. 3. R-factor, calculated for experimental and theoretical DEPES scans at $E_P=800$ eV, as a function of Ag domain populations n_1 and n_2. $R_{\min}$ equal to 0.29 was found for $n_1=75\%$ and $n_2=25\%$.

derivative with respect to the incidence angle Θ, respectively. Since the I values never reach zero the following R-factor was used:[37]

$$R = \int (L_{\mathrm{Th}} - L_{\mathrm{Ex}})^2 d\Theta \Big/ \int (L_{\mathrm{Th}}^2 + L_{\mathrm{Ex}}^2) d\Theta, \qquad (6)$$

where L_{Th} and L_{Ex} are I'/I ratios for theoretical and experimental data, respectively, and Θ is the polar angle.

In Fig. 3 the R-factor, calculated for experimental and theoretical DEPES scans at $E_P=800$ eV, is presented as a function of n_1 and n_2 populations. The minimum of the R value equal to 0.29 was found for $n_1=75\%$ and $n_2=25\%$. The theoretical DEPES profile obtained for the best fit and the corresponding experimental scan are shown in Fig. 4.

The calculated populations of rotated and unrotated Ag domains from DAES and DEPES obtained for different energies E_P are presented in Table I. The mean values of populations are $\overline{n_1}=71\pm3\%$ and $\overline{n_2}=29\pm3\%$, which demonstrates the preferred growth of one domain.

Different populations of rotated and unrotated domains with respect to Cu(111) are likely to be associated with atomic steps on the Cu(111) surface oriented along a certain direction, resulting from a miscut of the sample. The preferred occupation sites close to the atomic steps, as it occurs for an Ag/Cu adsorption system, extort the sequence of adatoms in an overlayer. Therefore the ABCBAC sequence can dominate in Ag layers. For Ag islands nucleating on flat Cu(111) terraces both ABCBAC and ABCABC sequences

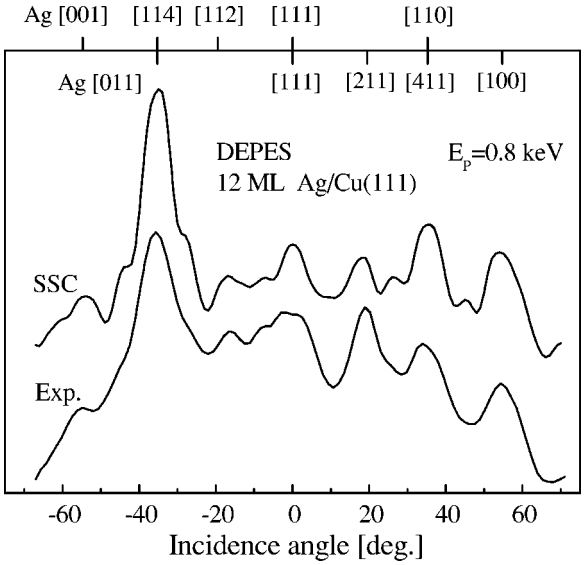

FIG. 4. Experimental DEPES scan for 12 ML of Ag on Cu(111) and $E_P=0.8$ keV in the $[11\overline{2}]$ azimuth of Cu and corresponding theoretical profile obtained for the best fit at $n_1=75\%$ and $n_2=25\%$ (Fig. 3).

are possible, which leads to the growth of rotated and unrotated domains.

Similar information concerning domain populations can be derived from the LEED patterns. To obtain this quantitative information from $I(V)$ curves the single domain intensity-energy spectrum of the appropriate diffracted beams from the Ag(111) crystal is required.

V. CONCLUSIONS

The comparison of experimental and theoretical results shows that the diffraction of primary electrons measured by DAES and DEPES reflects the crystalline structure of the sample. In spite of the fact that only single scattering of primary electrons was taken into account the main intensity maxima observed experimentally are predicted by the SSC theory. In view of this fact very useful quantitative information concerning domain populations can be obtained with the use of a R-factor analysis. The information depth depends on the inelastic mean free path of incident and emitted electrons. Experimentally, this is achieved by selecting the value of E_P and the measured electrons in DAES and DEPES.

ACKNOWLEDGMENTS

I wish to acknowledge the support of the University of Wrocław under grant 2016/W/IFD/04. I am indebted to Professor Stefan Mróz for helpful discussions and Zbigniew Jankowski for technical assistance.

*Electronic address: nowicki@ifd.uni.wroc.pl

[1] E. Bauer and J. H. van der Merwe, Phys. Rev. B **33**, 3657 (1986).
[2] C. Mottet, G. Tréglia, and B. Legrand, Phys. Rev. B **46**, 16018 (1992).
[3] C. S. Fadley, Prog. Surf. Sci. **16**, 275 (1984).
[4] C. S. Fadley, in *Synchrotron Radiation Research: Advances in Surface Science*, edited by R. Z. Bachrach (Plenum Press, New York, 1990).

[5] W. F. Egelhoff, CRC Crit. Rev. Solid State Mater. Sci. **16**, 213 (1990).
[6] S. A. Chambers, Adv. Phys. **40**, 357 (1991).
[7] H. P. Bonzel, Prog. Surf. Sci. **42**, 219 (1993).
[8] H. C. Poon and S. Y. Tong, Phys. Rev. B **30**, 6211 (1984).
[9] L. de Bersuder, C. Corotte, P. Ducros, and D. Lafeuille, in *The Structure and Chemistry of Solid Surfaces*, edited by G. A. Somorjai (Wiley, 30.1, New York, 1969).
[10] T. W. Rusch, J. P. Bertino, and W. P. Ellis, Appl. Phys. Lett. **23**, 359 (1973).
[11] G. Allié, E. Blanc, and D. Dufayard, Surf. Sci. **46**, 188 (1974).
[12] A. F. Armitrage, D. P. Woodruff, and P. D. Johnson, Surf. Sci. **100**, L483 (1980).
[13] Y. U. Idzerda and G. A. Prinz, Phys. Rev. B **43**, 11460 (1991).
[14] S. Mróz and M. Nowicki, Surf. Sci. **297**, 66 (1993).
[15] S. Valeri, A. di Bona, and G. C. Gazzadi, Surf. Sci. **311**, 422 (1994).
[16] S. Mróz, Surf. Rev. Lett. **4**, 117 (1997).
[17] S. Valeri and A. di Bona, Surf. Rev. Lett. **4**, 141 (1997).
[18] S. Valeri, Surf. Rev. Lett. **4**, 937 (1997).
[19] S. Mróz, Prog. Surf. Sci. **48**, 157 (1995).
[20] S. Mróz, H. Otop, and Z. Jankowski, Surf. Sci. **402**, 263 (1998).
[21] M. Nowicki and J. Osterwalder, Surf. Sci. **408**, 165 (1998).
[22] M. Nowicki, Vacuum **54**, 73 (1999).
[23] S. Mróz, M. Nowicki, and A. Krupski, Prog. Surf. Sci. **74**, 109 (2003).
[24] A. Stuck, M. Nowicki, S. Mróz, D. Naumović, and J. Osterwalder, Surf. Sci. **306**, 21 (1994).
[25] R. E. Weber and L. F. Cordes, Rev. Sci. Instrum. **37**, 112 (1966).
[26] S. Mróz, Vacuum **45**, 357 (1994).
[27] Y. Gao and J. Cao, Phys. Rev. B **43**, 9692 (1991).
[28] J. B. Pendry, *Low Energy Electron Diffraction* (Academic Press, London, 1974).
[29] D. J. Friedman and C. S. Fadley, J. Electron Spectrosc. Relat. Phenom. **51**, 689 (1990).
[30] J. J. Rehr and R. C. Albers, Phys. Rev. B **41**, 8139 (1990).
[31] W. E. McMahon, E. S. Hirschorn, and T. C. Chiang, Surf. Sci. **279**, L231 (1992).
[32] J. J. Lander, Phys. Rev. **91**, 1382 (1953).
[33] T. E. Gallon, Surf. Sci. **17**, 486 (1969).
[34] D. C. Jackson, T. E. Gallon, and A. Chambers, Surf. Sci. **36**, 381 (1973).
[35] C. Argile and G. E. Rhead, Surf. Sci. **53**, 659 (1975).
[36] G. E. Rhead, J. Vac. Sci. Technol. **13**, 603 (1976).
[37] J. B. Pendry, J. Phys. C **13**, 937 (1980).